Weidenfeller, Bernd; Rode, Hauke; Weidenfeller, Laura; Weidenfeller, Katrin:

Crystallinity, thermal diffusivity, and electrical conductivity of carbon black filled polyamide 46

Crystallinity, thermal diffusivity, and electrical conductivity of carbon black filled polyamide 46

Bernd Weidenfeller ®,[1] Hauke Rode,[1]* Laura Weidenfeller,[2] Katrin Weidenfeller[3]

[1]Department of Materials Science, Clausthal University of Technology, Arnold-Sommerfeld-Straße 6, 38678, Clausthal-Zellerfeld, Germany

[2]Institute of Process Measurement and Sensor Technology, Ilmenau University of Technology, Gustav-Kirchhoff-Straße 1, 98693, Ilmenau, Germany

[3]Medical University Varna, ul. Arhimandrit Filaret 9, 9001, Varna, Bulgaria

Correspondence to: B. Weidenfeller (E-mail: bernd.weidenfeller@tu-clausthal.de)

ABSTRACT: Polyamide 46 (PA 46) with carbon black (CB) has been subjected to a heat treatment. Crystallinity, specific heat capacity, crystalline melting peak temperature, thermal diffusivity, and electrical conductivity were measured. The crystallinity increases with duration of thermal treatment. The maximum value is dependent on the filler fraction. A lower CB content leads to a higher crystallinity at maximum tempering time. The crystalline melting peak temperature increases with decreasing filler fraction and duration of thermal treatment due to different crystal types and/or diverging geometric forms of the crystals. Thermal diffusivity and electrical conductivity act positively proportional to each other and increase with CB content and tempering time. The thermal diffusivity decreases with increasing temperature. The volume resistance of PA 46 is lowered by heat treatment. By CB addition in combination with a tempering process, the PA 46 can be transferred into a conductor. CB is moved by PA 46 crystals into amorphous regions forming conductive pathways. © 2019 The Authors. *Journal of Applied Polymer Science* published by Wiley Periodicals, Inc. J. Appl. Polym. Sci. **2020**, *137*, 48882.

INTRODUCTION

Thermoplastic polymers are more and more replacing conventional materials behaving as multifunctional materials. The low weight, the easiness in processing and the ability of tailoring various properties with or without use of filler materials make these materials advantageous. Especially, their use in electrical and thermal applications requires a thorough study of their properties.

There are several possibilities to increase thermal and/or electrical conductivity: Electrical and thermal conductivity of polymeric materials can be increased by the addition of suitable fillers and investigations on this topic can be found in numerous publications.[1–6] The resulting thermal and/or electric conductivity can be described by various mixing rules characterizing experimental results more or less satisfactory by using electrical and thermal conductivity values of the matrix and filler material.[4]

Carbon black (CB) is a suitable filler due to its low percolation threshold around 0.02–0.06 for low- and high-density polyethylene (LDPE and HDPE).[7,8] At low filler fractions below the percolation threshold, the electrical conductivity is comparable to the conductivity of the matrix polymer. Reaching the percolation threshold, the conductivity increases rapidly due to the forming of conductive pathways. In electric conductive polymer matrix composites, a significant increase in conductivity requires, therefore, a filler volume fraction exceeding the percolation threshold. Furthermore, the interconnectivity between filler particles is evident for the increase in electrical and thermal conductivity of polymer composites.[3,9,10]

However, also without any additional fillers, thermal and electrical conductivity can be increased. Mergenthaler *et al.* studied the increase in thermal diffusivity after orientation of polymer crystals by stretching which leads to a hundred times increase in

thermal diffusivity.[11] Pietralla showed that the mean free path of phonons is the limiting factor of thermal conductivity in polymers, and high conductivity can only be achieved for perfect crystalline materials minimizing boundary conditions at adjacent crystals.[12] Likewise, it was shown that also the crystalline structure influences the electric conductivity of neat polymers.[13,14] The electric transport in polymers may take place by moving charge carriers which can be either electrons, holes or ions. Ions can be trapped in the polymer during the preparation process and charge carriers can be injected from the contact electrodes into the polymer. The electric conductivity in polymers is determined by such impurities and therefore it is mainly dependent on the impurity concentration and its mobility. Because of the higher free volume in the amorphous phase compared to the crystalline areas, the mobility of the impurities is higher than in crystalline areas leading to higher electric conductivity in amorphous regions in comparison to crystalline areas. Regarding the mechanisms of charge transport in polymers, the reader may be referred to literature.[15,16]

In spite of the importance of polymers with high thermal and electrical conductivity in some technical areas, experimental measurement values show significant variation because the microstructures of the investigated polymers are not comparable. In this work, we therefore studied the influence of crystallinity of CB filled polyamide 46 (PA 46) changed by a thermal treatment on electrical and thermal properties. Furthermore, we investigated the temperature dependence of thermal diffusivity. We will show that an increase in size and perfection of crystalline areas in PA 46 leads to a rise of thermal diffusivity and simultaneously to a decrease in volume resistivity.

EXPERIMENTAL

Materials
As polymeric matrix an industrial available PA 46 (Stanyl TW341 by DSM, JH Heerlen, The Netherlands) was chosen. Some selected properties of the PA 46 are listed in Table I. The conductive filler was the CB Ensaco 250 G (IMERYS Graphite & Carbon, Bodio, Switzerland). The particle size distribution which can be seen in Figure 1 was measured by photon cross-correlation spectroscopy (Nanophox NX0108; Sympatec, Clausthal-Zellerfeld, Germany) in the measurement region from 30 to 4000 nm. A scanning electron microscopy picture of the CB taken with a DSM Gemini
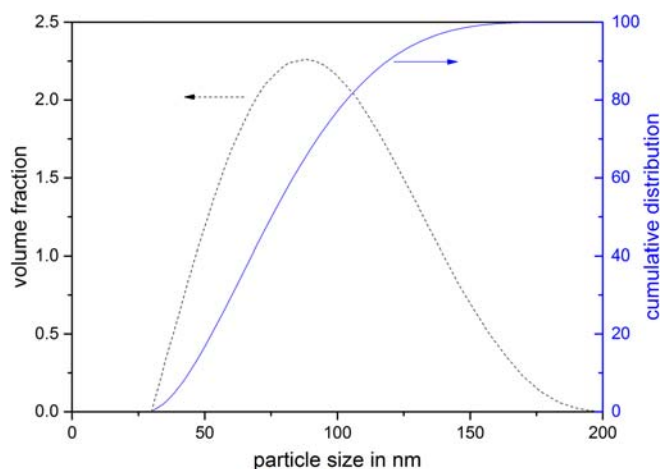

Figure 1. Particle size distribution and cumulative distribution of the CB Ensaco 250 G measured by photon cross correlation spectroscopy. [Color figure can be viewed at wileyonlinelibrary.com]

982 (Zeiss, Jena, Germany) is shown in Figure 2. The density of CB is $\varrho = 1.7$ g cm^{-3} (manufacturer's data). Because CB exists only in granular form by compression molding no data to thermal end electrical conductivity are available. Khizhnyak et al. measured a low thermal conductivity depending on particle sizes and compacting pressure on granular disc shaped samples between 0.18 W m^{-1} K$^{-1} \leq \lambda \leq 0.45$ W m^{-1} K^{-1}.[17] However, thermal conductivity was calculated to be $\lambda = 10^{10} - 10^{11}$ W m^{-1} K^{-1}.[18]

Sample Preparation
Samples with 10, 20, and 30-vol% CB in a PA matrix were prepared by extrusion compounding and injection molding. Before the compounding process, the PA was dried in an oven at 120 °C for 3 h. For extrusion compounding, a corotating twin-screw extruder of $D = 25$ mm diameter (ZE25-CL; Berstorff, Germany) with a length of 40D was used. The polymer pellets were fed gravimetrically (FlexWall 33; Brabender Technology, Germany) into the feed throat having room temperature. At the fifth zone of the

Table I. Selected Properties of the Polyamide Stanyl TW341 (tab: Stanyl-TW341)

Property	Symbol	Value	Unit
Density	ϱ	1.18	g cm^{-3}
Melting temperature	T_m	295	°C
Glass transition temperature	T_g	75	°C
CTE $T > T_g$, ‖ fiber axis		0.85×10^{-4}	°C^{-1}
CTE $T > T_g$, ⊥ fiber axis		1.2×10^{-4}	°C^{-1}
Volume resistivity	ρ	1×10^{-13}	Ω m
Surface resistivity	R_O	1×10^{-13}	Ω

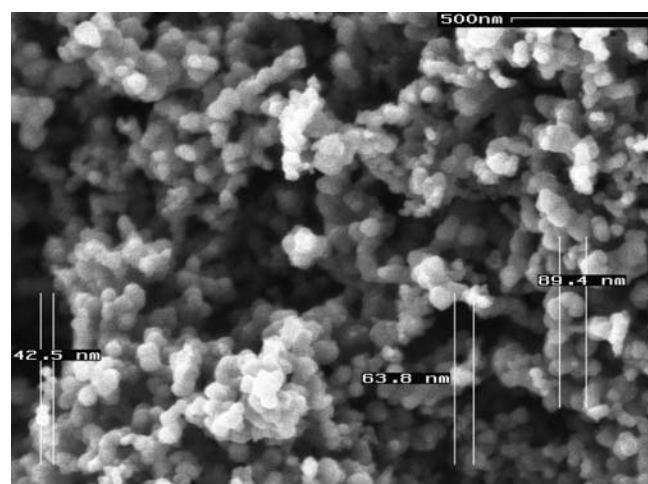Abbreviation: CTE, coefficient of thermal expansion.

Figure 2. Scanning electron microscope image of the CB Ensaco 250 G with indication of particle sizes.

extruder a side feeder (ZSFE) was mounted, which receives the CB from another gravimetric dosing system (Soder T20; K-Tron Deutschland GmbH, Germany) and feeds it into the molten polymer. Temperatures in the different zones of the extruder were ranging from 280 to 300 °C (temperatures of Zones 1–8: 280, 285, 285, 290, 295, 295, and 300 °C). The compound left the extruder passing a plate (300 °C) with two holes of 4 mm diameter. The strands were cooled in a water bath (20 °C) and pelletized afterward.

After another drying step of 3 h at 80 °C, two discs of d = 25.4 mm diameter and t_1 = 1 mm and t_2 = 2 mm thickness together with two parallelepipeds with l = 30 mm length, w = 10 mm width, and t_3 = 3 mm thickness in one mold were prepared using an injection molding machine (Allrounder 220S 150-60, Arburg, Germany). The feeding zone was at room temperature, Zones 1–3 had temperatures of 290, 295, and 300 °C and the temperature at the nozzle was 310 °C. The mold was at room temperature.

Thermal treatments of the samples at a temperature of T = 260 °C for various times (0, 1, 2, 4, 16, 32, 64, and 128 h) were done in an oven (Nabertherm, Lilienthal, Germany) under argon atmosphere with an argon volume flow of 1 L min^{-1}. The oven was heated to a constant temperature of 260 °C before the samples were put into the oven. After end of annealing time, the cooling of samples was done at air.

Therefore, cooling and heating times for samples were not exactly estimated but they can be calculated by knowledge of thermal diffusivity, samples thickness, and start and end temperatures using formulas given in a previous paper.[19] Taking sample sizes and a thermal diffusivity of 0.15 mm^2 s^{-1} for the neat polymer, the time for reaching the oven temperature of 260 °C is below 30 s, and for CB filled samples significant lower. The error in time for the shortest annealing time of 1 h is therefore less than 1%.

Experimental Methods

The temperature-dependent thermal diffusivity $\alpha(T)$, which is correlated with thermal conductivity $\lambda(T)$, specific heat capacity $c_p(T)$, and specific density $\rho(T)$ by the relation $\alpha = \lambda/(c_p\rho)$, was investigated in a laser flash apparatus (LFA 427; Netzsch-Gerätebau GmbH, Selb, Germany) from 300 to 530 K under helium atmosphere. Samples were covered by a thin graphite layer to ensure a good absorption of the laser light and to prevent damage by the laser pulse. The curves of the detector signals after the laser pulse showed the best fit with the applied Cowan model.[20] Shown measurement values are the average values of three measurements. The accuracy of this measurement method is better than 3%.

Using a differential scanning calorimeter DSC 204 F1 2920 (Netzsch-Gerätebau GmbH), the specific heat capacity, crystallinity, glass transition temperature, and melting temperature were measured. Measurements were carried out from 300 to 700 K with a heating rate of 10 K min^{-1}. The differential scanning calorimeter was calibrated in the same temperature range using sapphire (Al$_2$O$_3$) sample as standard. The accuracy of the measurements is better than 3%. Peaks in DSC curves were fitted with PeakFit v4.02 software (Jandel Scientific Software).

Measurements of the resistivity were done with an Agilent 4339B High Resistance meter for neat PA46 samples and PA + 10-vol%
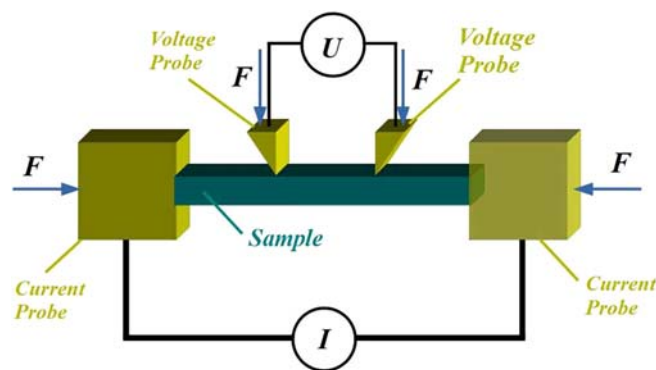

Figure 3. Schematic representation of the four-probe measurement setup. [Color figure can be viewed at wileyonlinelibrary.com]

CB samples while PA samples filled with 20-vol% and 30-vol% CB with a higher electrical conductivity were measured with an Agilent 34401A digital multimeter in four-probe measurement technique. A schematic drawing of the measurement setup can be seen in Figure 3 which shows the traditional geometry for direct current conductivity measurements.[21] All probes were pressed with a force of F = 34.1 kN onto the sample. To eliminate contact resistances, four measurements with reversed polarities of current and voltage probes were taken 30 s after the current was switched on. The resistance value is the average value of all measurements. Prior to the measurements, the surfaces of the samples were cleaned with sandpaper to remove the thin polymer skin occurring in the injection molding process and afterward the sample dimensions were taken with an accuracy of 0.001 mm. The distances between knife-edges of voltage probes were 10 mm, and distances between current probes and knife edges were also 10 mm. Inhomogeneities in the sample are averaged out by the relatively large size of the sample. The maximum systematic error of these measurements is below 4%.

The morphology of CB and of PA-CB composites were investigated with a high-resolution scanning electron microscope (Carl Zeiss DSM 982 Gemini).

RESULTS AND DISCUSSION

Crystallization Behavior

Figure 4 shows the DSC curves of the PA with and without CB filler after various annealing times between 0 and 128 h at 260 °C. It is clearly visible that an elongation of annealing time leads to a shift of the melting peak to higher temperatures. Regarding the DSC curve of the neat PA, a peak with a low shoulder at the low temperature side is visible. The first annealing procedure of 1 h leads to an increase of the peak in which the low temperature shoulder is integrated. This means an increase of the overall crystallinity of the sample. Annealing times of 2 and 4 h induce a shift of the melting peak to higher temperatures which is generally an indication for an increase in size and perfection of the crystals. After an annealing time of 8 h, again, a clear and nearly separated low temperature shoulder is developed. Furthermore, a splitting of the high temperature peak in a clear double peak is visible, which is especially evident in the DSC curve of the 64 h annealed neat PA [cf. Figure 4(a)]. Together
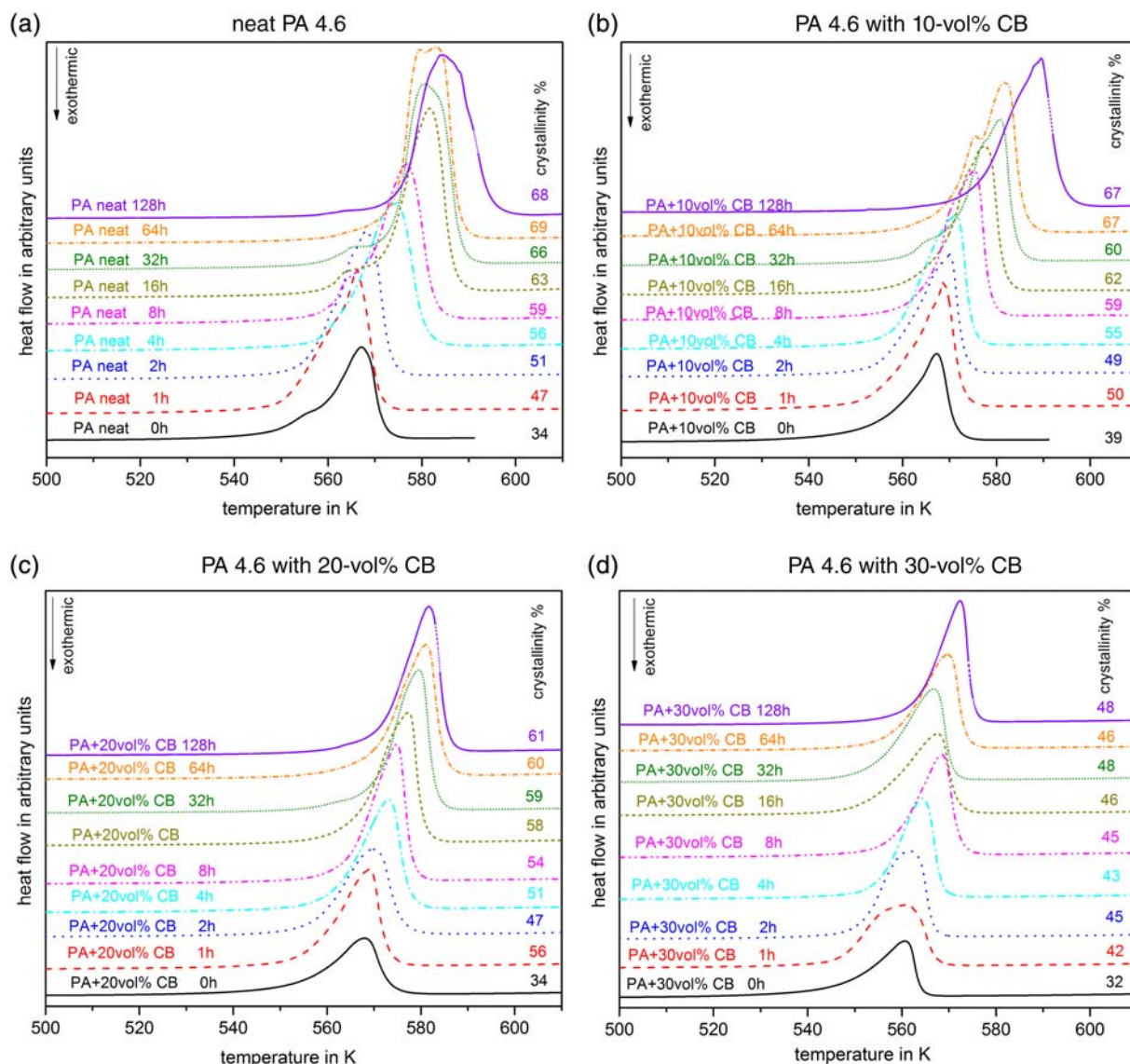
Figure 4. DSC curves of the PA 46 with various amounts (0, 10, 20, and 30 vol %) CB filler after heat treatment at 260 °C for 0, 1, 2, 4, 8, 16, 32, 64, and 128 h annealing time. [Color figure can be viewed at wileyonlinelibrary.com]

with the low temperature shoulder, the melting peak of neat PA and PA with 10-vol% CB can be subdivided into three clear peaks using PeakFit software for annealing times above 32 h, while for all other samples only a subdivision into two peaks was found.

A clear double peak was also found by Gaymans *et al.* in a rapidly quenched sample which leads to the assumption of two different crystals varying in their melting temperatures.[22] In crystallization experiments at 280 °C, Ramesh showed the development of a crystallization in hexagonal structure, and the peak is growing with annealing time indicating an increase in crystallinity.[23] By cooling down from the crystallization temperature at 280 °C, the evolution of a second peak was observed which can be attributed to the crystalline α-phase. Conversely, the transition from the α-phase into the hexagonal crystalline phase can be observed by heating. Finally, also at much lower temperatures, another crystalline transition from a high temperature α phase into a low temperature α-phase was found.[24] Using a

crystallization temperature of 260 °C, the transitions appear at 110 and 220 °C, respectively.[23] The Brill temperature at which the transition from high temperature α-phase into hexagonal crystal structure appears is around 245 °C while for annealing temperatures between 180 and 240 °C an intermediate pseudohexagonal phase is formed.[25–27]

It should be mentioned here that also the influence of annealing time on the crystallinity was investigated for other polymers like HDPE.[28] It was found that the annealing at a temperature close below crystalline melting temperature led to an additional melting peak at lower temperature.[28] This new peak was explained by the lamellar thickening leading to an increase in crystallinity of 4% and increase of crystalline melting temperature of 3.1 K.

A similar evolution of the peak temperatures with the annealing time can be seen for all investigated samples in Figure 5. The peak temperature of the low temperature shoulder P_{LT} of the low
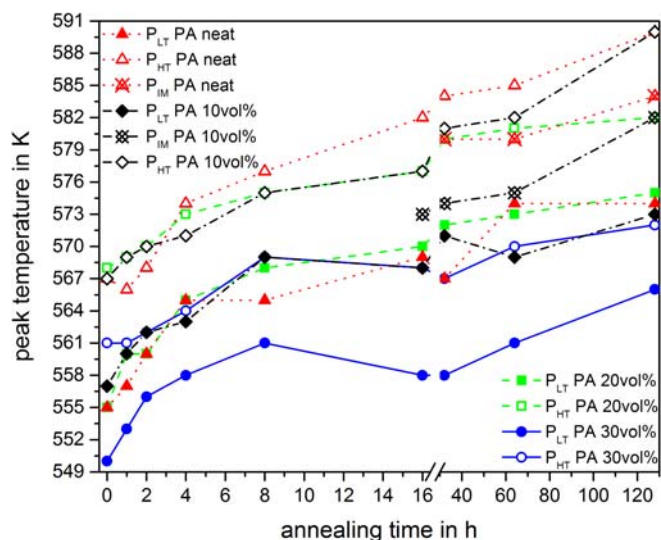
Figure 5. Evolution of the peak temperatures of melting peaks seen in DSC curves of the PA 46 with various amounts (0, 10, 20, and 30 vol %) CB filler after heat treatment at 260 °C for 0, 1, 2, 4, 8, 16, 32, 64, and 128 h annealing time. The peak temperatures were found by fitting DSC curves (cf. Figure 3) with PeakFit software. P_{LT}, P_{HT}, and P_{IM} stand for the peak temperature of the low temperature shoulder, the high temperature peak, and an intermediate peak, respectively. [Color figure can be viewed at wileyonlinelibrary.com]

temperature melting peak (filled triangles) lies for the injection molded neat PA sample at 555 K (0 h annealing). With increasing annealing time it is increased up to 574 K. Simultaneously, the peak temperature of the high temperature melting peak P_{HT} (open triangles) is increased from 576 to 590 K. After an annealing time of 32 h additionally to the low temperature shoulder P_{LT}, a high temperature double (intermediate) peak P_{IM} (crossed triangle) develops which is present also in the 64 and 128 h annealed samples. Also Derks _et al._ found an increase in peak temperatures of Nylon 46 annealed at 260 °C, which is for the high temperature peak and for annealing times of 0, 2, 4, and 20 h nearly identical to the here shown values while for the low temperature peak no data are given.[29]

Generally, a shift of the melting peak to higher temperatures indicates an increase in size and perfection of the crystals.[22] In our investigation, the annealing temperature lies above the Brill temperature of 245 °C and therefore an increasing perfection of hexagonal structure is more likely than a change from α-phase into hexagonal phase. However, it can be assumed that the transformation of the α-phase into the hexagonal phase is incomplete at the beginning of our annealing experiments and that the transformation proceeds during annealing time. Thus, the low temperature shoulder P_{LT} might be attributed to the α-phase which is transformed into the hexagonal phase by proceeding annealing time generating the high temperature peak P_{HT}. This assumption is supported by the fact that the peak temperature of the low temperature peak (shoulder) P_{LT} lies at 574 K after an annealing time of 128 h, which is just the temperature of the high temperature peak P_{HT} at 0 h annealing. Furthermore, the presence of the double peak (cf. Figures 4 and 5) which consists of the intermediate peak P_{IM} (crossed triangles) and the high

temperature peak P_{HT} which appears for annealing times of 32 h and more indicates the existence of two different crystal structures. This intermediate peak might be attributed to the intermediate pseudohexagonal phase.[26,27]

Similar observations can be made for the PA samples with 10-vol % CB filler whereas the intermediate peak P_{IM} (crossed black diamonds) can already be found after 16 h of annealing time. Regarding a slight scatter in the peak temperatures, the peak temperatures of the low temperature peak P_{LT} (filled diamonds) and the high temperatures peak P_{HT} (open diamonds) of the neat PA samples and the PA samples with 10-vol% CB filler are nearly of the same height, while the peak temperatures of the intermediate peak P_{IM} are significant below the peak temperatures of the neat polymer. However, after an annealing time of 128 h, the peak temperatures are approximating which indicates a hindrance of the intermediate phase by the CB filler which can be overcome at long annealing times.

Also the low temperature peak P_{LT} (filled squares) and the high temperature peak (open squares) of the PA with 20-vol% filler are within a slight scatter at the same temperatures as for unfilled and with 10-vol% CB filled PA, while the peak temperatures (P_{LT}: filled circles; P_{HT}: open circles) for the PA with 30-vol% CB are significantly lower. This indicates a hindrance for the growth and perfection of the crystals which might be due to the percolation of the CB filler which appears for ideal monosized spherical particles at a theoretical percolation threshold at a filler fraction of around 30 vol%.[3]

Additionally, Figure 4 shows that the crystallinity of all samples is increased with the duration of the heat treatment. The crystallinity increased very fast from an annealing time of 0 h to an annealing time of 64 h. For example, the data measured for the neat PA shows a crystallinity of 34% without heat treatment and rises up to 69% after 64 h annealing time. A variation of the heat treatment duration from 64 to 128 h recorded just small changes in crystallinity. After an annealing time of 32 h, a crystallinity of 59% is observed which is just the identical value which was found by Yamanobe _et al._ after a crystallization time of 24 h.[30] If 10-vol % CB is added, the crystallinity of the injection molded sample without a heat treatment is increased up to 39%. It seems as if the CB filler acts as a nucleating agent for crystals. A similar observation was made for CB as a filler in PA 66 or for carbon nanotubes in PA 46.[5,31]

With increasing annealing time, the maximum crystallinity is with 67% in the same range as for the neat PA 46. If the amount of CB filler is raised to 20 and 30 vol%, the crystallinity is reduced compared to the neat PA and the PA with 10-vol% CB for the not heat-treated material as well as for the annealed PA 46. This might be due to a diminished space in which the PA crystals can accumulate because an increased volume is occupied by the CB.

Thermal Diffusivity

Figure 6 shows the dependence of thermal diffusivity of neat PA samples after various annealing times. It can be seen that the thermal diffusivity is decreased with increasing temperature. This behavior was previously observed also for other polymers like
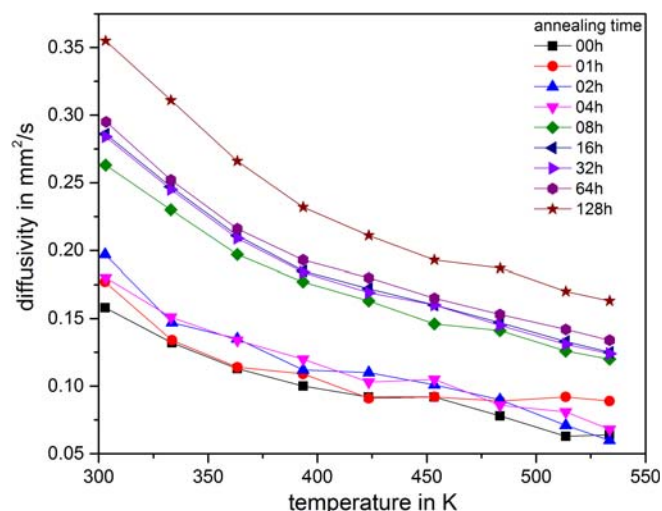
Figure 6. Temperature dependence of thermal diffusivity of neat PA after various annealing times. [Color figure can be viewed at wileyonlinelibrary.com]
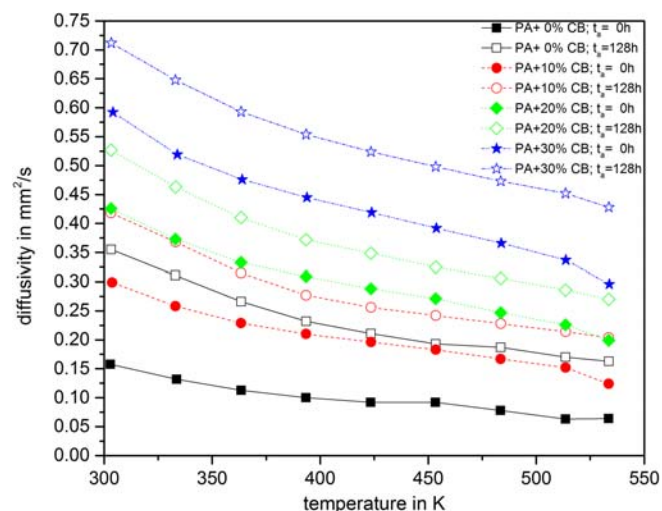

Figure 7. Dependence of thermal diffusivity on the temperature, annealing time and CB filler content. For the purpose of clarity, only data of not annealed and 128 h annealed samples are shown. Additionally, measured data can be found in Table II. [Color figure can be viewed at wileyonlinelibrary.com]

polypropylene and is explained by the decrease in mean free path of phonons.[4,32,33] Furthermore, it can be seen that the thermal diffusivity is more than doubled with an annealing time of 128 h from $\alpha_{neat,0\ h} = 0.158$ mm^2 s^{-1} to $\alpha_{neat,128\ h} = 0.355$ mm^2 s^{-1}. It can be assumed that this is due to the increase in perfection of the crystals. A similar result, namely, the increase in thermal diffusivity was already observed for ultraoriented polyethylene and for PA6 filled with graphite nanoplatelets and single wall carbon nanotubes.[11,34] Also, Pietralla showed that the limiting factor in thermal conductivity of materials is the mean free path of phonons in polymers.[12] He explained that the thermal diffusivity can be dramatically enhanced by a perfection of the crystalline structure of a polymer.

A further increase of the thermal diffusivity is feasible by the addition of a thermally conductive second phase like CB as it can

be seen in Figure 7. For the purpose of clarity, not all measured values are shown in Figure 7, but they can be seen in Table II. It is observable that the thermal diffusivity is increased by the addition of CB in the whole measured temperature range compared to the neat PA ($\alpha_{0\ h,0\%CB,300\ K} = 0.158$ mm^2 s^{-1}) without annealing. However, the neat PA annealed for 128 h ($\alpha_{128\ h,0\%CB,300\ K} = 0.355$ mm^2 s^{-1}) has a higher thermal diffusivity than the PA filled with 10-vol% CB without annealing ($\alpha_{0\ h,10\%CB,300\ K} = 0.299$ mm^2 s^{-1}). This behavior indicates that the annealing of the PA followed by a perfection of crystals is more effective to increase thermal diffusivity than the addition of a small amount of CB filler. The highest thermal diffusivity was measured for PA filled with 30-vol% CB annealed for 128 h with $\alpha_{128\ h,30\%CB,300\ K} = 0.712$ mm^2 s^{-1} which is 4.5 times higher than the thermal diffusivity of the not annealed neat PA.

Previously, it was shown that the addition of metallic (FeSi) and diamond particles increase the thermal diffusivity of polymer matrix composites whereas the addition of these particles increases significantly the mean free path of phonons.[6,33] Furthermore, it was shown that smaller particles of the same filler lead to higher thermal diffusivity than larger particles.[35] In the present study, nanoparticles were used and the high filler fraction together with the high crystallinity indicate a good conductive network.

Volume Resistance

In Figure 8, the dependence of the volume resistance on the annealing time with and without CB filler content after a heat treatment at 260 °C in argon atmosphere can be seen. It is evident that the volume resistance for all samples decreases with increasing heat treatment duration. The volume resistance of the neat PA falls from above 1×10^{15} Ωmm before annealing to approximately 3×10^{11} Ωmm after a heat treatment of 128 h. The decrease in volume resistance of the neat PA samples in low tempering time (0–32 h) is almost not noticeable, while there is a larger decrease in resistance from 32 to 64 h. The largest decrease can be seen between annealing times of 64 and 128 h. In general, the decrease of the measured resistivity is more pronounced for longer heat treatment times. As aforementioned, the conductivity in neat PA is caused by impurities which possess a higher mobility in the amorphous regions of the polymer than in the crystalline parts. Thus, it can be concluded that the creation of larger crystalline areas by the heat treatment leads to conductive pathways for the impurities in the amorphous parts resulting in a higher electrical conductivity. CB filled samples show a contrasting curve. The decrease of the volume resistance can be described as hyperbolic like. With increasing heat treatment duration, the volume resistance decreases by an ever-lower value. The samples of the PA 4.6 with 10-vol % CB show the highest variation in volume resistance of more than 10^8 Ωmm. It decreases from approximately 1×10^{13} Ωmm without annealing to about 5×10^4 Ωmm after an annealing time of 128 h.

This strong decrease might be explained by exceeding the percolation threshold which is reduced by the formation of more perfect crystals. There is not enough space for CB particles within the polymer crystals. By perfecting the crystal structure by annealing, the CB particles are moved into the amorphous region

Table II. Temperature-Dependent Thermal Diffusivity Values of PA 46 Filled with 0, 10, 20, and 30 vol % CB after Various Annealing Times t_a in Argon Atmosphere

t_a	Temperature (°C)	0 h	1 h	2 h	4 h	8 h	16 h	32 h	64 h	128 h
Neat PA 46	30	0.158	0.177	0.197	0.180	0.263	0.286	0.284	0.295	0.355
	60	0.132	0.134	0.147	0.151	0.230	0.247	0.245	0.252	0.311
	90	0.113	0.114	0.135	0.134	0.197	0.211	0.209	0.216	0.266
	120	0.100	0.109	0.112	0.120	0.177	0.185	0.184	0.193	0.232
	150	0.092	0.091	0.110	0.103	0.163	0.172	0.169	0.180	0.211
	180	0.092	0.092	0.101	0.105	0.146	0.160	0.160	0.165	0.193
	210	0.078	0.089	0.090	0.086	0.141	0.147	0.145	0.153	0.187
	240	0.063	0.092	0.071	0.081	0.126	0.133	0.131	0.142	0.170
	260	0.064	0.089	0.060	0.068	0.120	0.125	0.124	0.134	0.163
PA 46 + 10% CB	30	0.299	0.313	0.314	0.337	0.348	0.364	0.402	0.398	0.418
	60	0.258	0.270	0.264	0.287	0.296	0.308	0.355	0.354	0.368
	90	0.229	0.240	0.236	0.250	0.256	0.265	0.312	0.305	0.315
	120	0.210	0.222	0.217	0.231	0.235	0.240	0.279	0.269	0.277
	150	0.196	0.207	0.202	0.217	0.220	0.226	0.264	0.249	0.256
	180	0.183	0.190	0.192	0.202	0.204	0.212	0.251	0.233	0.242
	210	0.167	0.176	0.175	0.189	0.189	0.201	0.234	0.218	0.228
	240	0.152	0.163	0.155	0.175	0.177	0.184	0.223	0.206	0.214
	260	0.124	0.138	0.133	0.144	0.154	0.165	0.210	0.195	0.204
PA 46 + 20% CB	30	0.426	0.450	0.464	0.476	0.484	0.494	0.529	0.529	0.527
	60	0.373	0.389	0.399	0.413	0.423	0.431	0.459	0.464	0.463
	90	0.333	0.350	0.354	0.369	0.372	0.378	0.403	0.409	0.410
	120	0.309	0.322	0.331	0.344	0.345	0.346	0.366	0.372	0.372
	150	0.288	0.304	0.309	0.323	0.323	0.325	0.348	0.352	0.349
	180	0.271	0.284	0.290	0.303	0.301	0.305	0.328	0.329	0.325
	210	0.247	0.263	0.268	0.283	0.283	0.287	0.307	0.312	0.306
	240	0.226	0.245	0.244	0.261	0.262	0.266	0.287	0.290	0.286
	260	0.199	0.208	0.211	0.236	0.243	0.253	0.267	0.269	0.270
PA 46 + 30% CB	30	0.592	0.612	0.604	0.637	0.642	0.677	0.664	0.672	0.712
	60	0.519	0.536	0.528	0.560	0.563	0.597	0.589	0.596	0.648
	90	0.476	0.492	0.488	0.508	0.508	0.538	0.532	0.535	0.593
	120	0.445	0.461	0.456	0.481	0.476	0.502	0.496	0.500	0.554
	150	0.419	0.436	0.429	0.454	0.447	0.476	0.466	0.473	0.524
	180	0.392	0.411	0.403	0.426	0.421	0.449	0.442	0.443	0.498
	210	0.366	0.383	0.376	0.401	0.395	0.422	0.416	0.420	0.473
	240	0.337	0.352	0.347	0.369	0.366	0.395	0.389	0.395	0.452
	260	0.296	0.305	0.310	0.337	0.331	0.361	0.363	0.369	0.428

of the polymeric matrix forming there conductive pathways. PA46-10 vol % CB composite without annealing has a crystallinity of 39% while crystallinity is increased to 67% after 64 h annealing. Thus, the space for the CB particles in the amorphous region is nearly halved. This means that the CB fraction in amorphous region is doubled to 20 vol %. In fact, after an annealing time of 128 h, the volume resistance of PA46 + 10 vol % is comparable to the PA46 filled with 20 vol % CB. The evolution of a CB network was also found by Ren *et al*. during measurements of electrical conductivity in a rheometer.[36] However, the temperature lay in their measurements with 160 °C above the melting temperature and the plates of the rheometer were used as electrodes. Also, Liang concluded from resistivity and calorimetry measurements that a conductive network of carbon particles was formed during crystallization process in HDPE.[37] It was supposed that CB particles were discharged from crystalline areas and enriched in amorphous areas of the polymer during crystallization process. Previously, Song and Zheng found a formation of conductive network of CB particles in HDPE close below and also close above crystalline melting temperature.[28] In accordance

with our results, also Traina *et al.* found a decrease of volume resistance of CB filled HDPE with increasing duration of annealing at a temperature close to the crystalline melting temperature due to the formation of a conductive network of CB particles.[38] As we do, they also found that the thermal treatment is more effective than the increase of filler fraction in the composite.

The data of PA 4.6 filled with 20 and 30 vol % show an obvious fall from annealing times of 0 h to annealing times of 8 h. After a heat treatment of 8 h, the curves do not change dramatically anymore but are approaching their asymptotes. Not heat-treated samples of PA 4.6 with 20 vol % show values of volume resistance of roughly
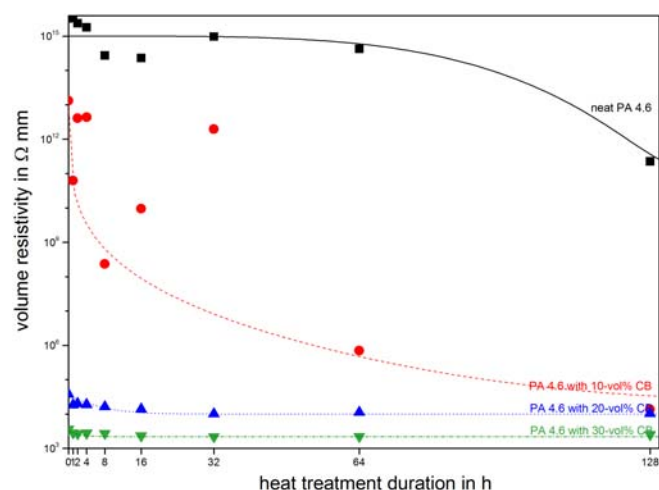
3.8×10^4 Ωmm which fall to about 1×10^4 Ωmm while the not tempered samples of PA 4.6 with 30 vol % show values of approximately 3.6×10^3 Ωmm which roughly fall to 2.5×10^3 Ωmm.

Morphology

Figure 9 shows the morphology of selected samples representing all investigated composites. In Figure 9(a), the PA 46 sample filled with 20 vol % CB before annealing is shown. The CB particles are homogeneously distributed in the sample by the preparation process. This can be seen by a comparison of Figure 9 (a) with Figure 2. While in Figure 2 agglomerates of the CB particles can be seen, these agglomerates were broken up. After 2 h annealing in argon atmosphere in Figure 9(b) a new agglomeration of the CB particles can be seen. These new agglomerates are forming conductive pathways. This formation of these conductive pathways leads to the increase in thermal diffusivity which can be seen in Figure 5 and the reduction of the volume resistivity which is shown in Figure 8. A significant improvement of the network formation in Figure 9(c–f) is not obvious. However, from Figure 8, it can be deduced that the network formation appears in the first hours of annealing process leading to a significant reduction of volume resistivity while it is less important for longer times. Thus, no substantial changes in the network formation of CB particles can be seen.

CONCLUSIONS

Both thermal diffusivity and electrical conductivity of PA4.6 can be significantly increased by a thermal treatment after an injection molding of samples. An uncompleted transformation of the α-phase into the hexagonal phase is promoted by the heat treatment. Additionally, the size and perfection of the crystals are improved. The changes in the crystalline part of the polymer lead to an increase of thermal diffusivity of more than twice as much as in the injection molded state after the heat treatment at
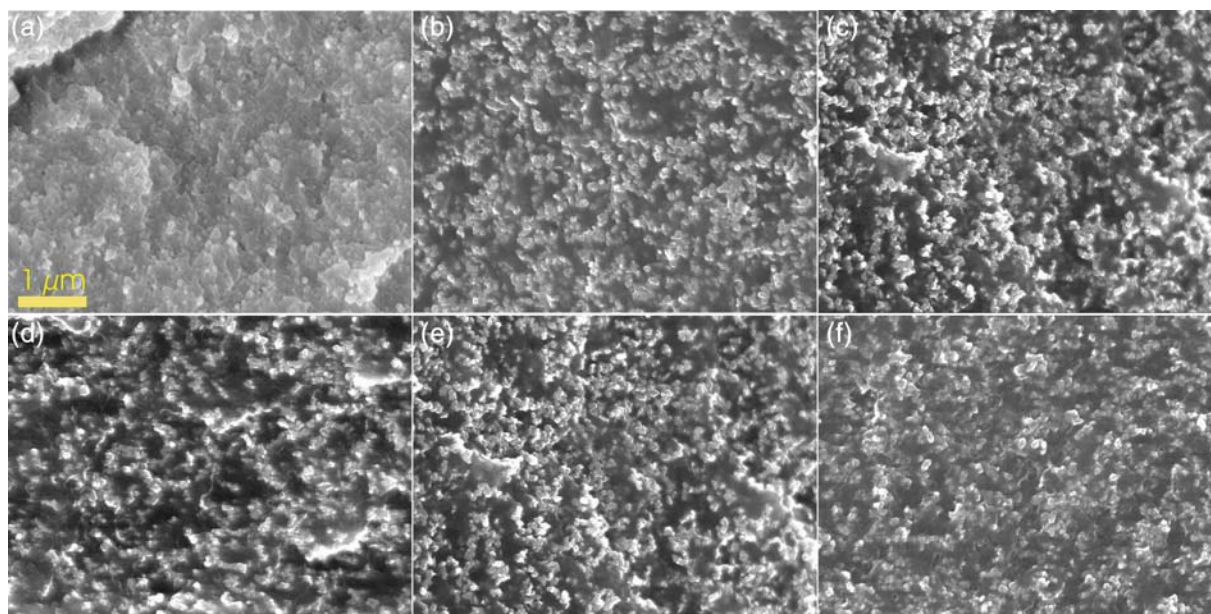

Figure 8. Dependence of the volume resistance on the annealing time and CB filler content (0, 10, 20, and 30 vol %) at 260 °C in an argon atmosphere. Exponential functions are added to lead the gaze. [Color figure can be viewed at wileyonlinelibrary.com]

Figure 9. Scanning electron micrographs of PA 46 filled with 20 vol % CB particles (a) after 0 h, (b) after 2 h, (c) after 8 h, (d) after 16 h, (e) after 64 h, and (f) after 128 h annealing at 260 °C in argon atmosphere. [Color figure can be viewed at wileyonlinelibrary.com]

260 °C for 128 h. The reason for the increase in thermal diffusivity is the decreasing number of scatter centers due to less boundaries in and between crystals. In PA-CB composites, additional thermally conductive pathways exist between CB particles.

Thermal diffusivity values of polymers after an annealing procedure are rarely found in literature. Neat PA 6 and PA 6 filled with graphite nanoplates, single walled carbon nanotubes and both fillers with filler fractions up to 50 wt % annealed at 150 °C for 0–50 h show thermal diffusivities values ranging from $\alpha \approx 0.2$ mm^2 s^{-1} to $\alpha \approx 5.5$ mm^2 s^{-1}.[34] Measurements on ultraoriented linear LDPE and LDPE revealed $\alpha \approx 0.2$ mm^2 s^{-1} but after stretching, the thermal diffusivity parallel to stretching direction increased up to $\alpha \approx 10$ mm^2 s^{-1} while it decreased in perpendicular direction to $\alpha \approx 0.08$ mm^2 s^{-1}.[11] Also, for neat polypropylene, a thermal diffusivity of $\alpha \approx 0.2$ mm^2 s^{-1} was reported while it can be increased up to $\alpha \approx 2.2$ mm^2 s^{-1} with various fillers without a heat treatment, whereas the interconnectivity of the filler particles plays a crucial role.[3,32] For neat polyurethane, a thermal diffusivity value of $\alpha \approx 0.18$ mm^2 s^{-1} was found which was increased by magnetite filler up to $\alpha \approx 0.33$ mm^2 s^{-1}.[35] Using diamond and iron particles as filler, the thermal diffusivity of polypropylene could be increased to $\alpha \approx 1.4$ mm^2 s^{-1}.[6] Thus, increasing thermal diffusivity by using an appropriate filler and a high filler volume fraction is an effective way to increase the thermal diffusivity of polymers. Nevertheless, the use of a low filler fraction in a semicrystalline polymer in combination with a thermal treatment as shown in this investigation leads to adequate thermal diffusivity values by forming a filler particle network.

Subsequently, also the electrical resistance is decreased for more than three orders of magnitude from around 10^{15} to 10^{12} Ωmm in the neat polymer. Due the improvement of size and perfection of crystals in thermal treatments, the CB particles are moved out of crystalline regions into amorphous regions of the polymer. Here, the relative filler fraction is increased forming conductive pathways in the amorphous parts of the polymer leading to resistivity around 10^3 Ωmm for heat-treated PA 46 filled with 30% CB.

Similar values for electrical resistance of neat and particulate filled polymers were reported in literature: For neat LDPE, a resistivity of around 10^{12} Ωmm was found which was reduced to values around 1–10^2 Ωmm for graphite filled LDPE and HDPE.[39] Values of 10^{14}–10^{15} Ωmm were found for neat LDPE and of 10^0–10^2 Ωmm for LDPE filled with various CB grades.[36,37,40] A higher resistivity around 10^{17} Ωmm of neat HDPE and a reduction to 10^0 Ωmm for CB filled HDPE was found by Ha et al.[38] During an isothermal annealing, the resistivity can be further reduced due to a network formation.[38] Comparable values were also found for PP filled with magnetite.[3] The reduction of the electrical resistivity was always explained by the formation of a conductive network whose absolute values depend on the filler fraction and the quality of the particle's interconnectivity.[3]

In this work, we could show that thermal and electrical conductivity of neat PA 46 and PA 46-CB composites can be dramatically improved by heat treatments.

Furthermore, we have seen that various annealing times lead to different crystalline phases and to different amounts of these phases after annealing procedure. For example, in neat PA

46 and in PA 46 with 10% CB, an intermediate pseudohexagonal phase can be observed which was not detected in composites with higher CB content. Thus, the question arises in which way the electrical conductivity and thermal diffusivity is influenced by crystalline phase. Furthermore, the influence of the intermediate pseudohexagonal phase on the properties of the PA 46-CB composites for CB content less than 10% could be investigated. Thus, the investigation of PA 46 CB composites with carbon content less than 10% and annealing temperatures promoting the various crystal structures as described previously should be done.

Summarizing it can be stated that already relative short thermal treatments of 8 h lead to a significant improvement of thermal diffusivity of neat PA46. Thus, compared to the addition of fillers, this opens a possibility of an improvement without dramatic changes in the weight of the polymer. The effect is even higher for longer times of thermal treatments and for PA46-CB composites. For increasing the electrical conductivity of neat PA46, a thermal treatment is less effective because much longer times for a thermal treatment are needed. Nevertheless, for composites of PA46 with a low amount of CB filler, a thermal treatment of 8–16 h also leads to a significant reduction of electrical resistivity. Thus, a thermal treatment of PA46-CB composites is an effective method to change thermal and electrical properties.

REFERENCES

1. Agari, Y.; Ueda, A.; Nagai, S. *J. Appl. Polym. Sci.* **1991**, *43*, 1117.

2. King, J. A.; Tucker, K. W.; Vogt, B. D.; Weber, E. H.; Quan, C. *Polym. Compos.* **1999**, *22*, 643.

3. Weidenfeller, B.; Schilling, F. R.; Höfer, M. *Compos. Part A.* **2002**, *33*, 1041.

4. Anhalt, M.; Weidenfeller, B. *J. Appl. Polym. Sci.* **2011**, *119*, 732.

5. Chiu, F.-C.; Kao, G.-F. *Compos. Part A.* **2012**, *43*, 208.

6. Weidenfeller, B.; Kirchberg, S. J. *Compos. Part B.* **2016**, *92*, 133.

7. Chodak, I.; Krupa, I. *J. Mater. Sci. Lett.* **1999**, *18*, 1457.

8. Clingerman, M. L.; King, J. A.; Schulz, K. H.; Meyers, J. D. *J. Appl. Polym. Sci.* **2002**, *83*, 1341.

9. Droval, G.; Feller, J. F.; Salagnac, P.; Glouannec, P. *Polym. Adv. Technol.* **2006**, *17*, 732.

10. Im, H.; Kim, J. *Carbon.* **2011**, *49*, 3503.

11. Mergenthaler, D. B.; Pietralla, M.; Roy, S.; Kilian, H.-G. *Macromolecules.* **1992**, *25*, 3500.

12. Pietralla, M. *J. Comp. Aided Mater. Des.* **1996**, *3*, 273.

13. Yoshino, K.; Yin, X. H.; Tada, K.; Kawai, T.; Hamaguchi, M.; Araki, H. *IEEE Trans. Dielectr. Electr. Ins.* **1996**, *3*, 331.

14. Kim, D.; Yoshino, K. *J. Phys. D: Appl. Phys.* **2000**, *33*, 464.

15. Lewis, T. J. *J. Phys. D: Appl. Phys.* **1990**, *23*, 1469.

16. Teyssedre, G.; Laurent, C. *IEEE Trans. Dielectr. Electr. Ins.* **2005**, *12*, 857.

17. Khizhnyak, P. E.; Chechetkin, A. V.; Glybin, A. P. *J. Eng. Phys.* **1979**, *37*, 1073.

18. Agari, Y.; Uno, A. *J. Appl. Polym. Sci.* **1986**, *32*, 5705.

19. Weidenfeller, B.; Schilling, F.; Höfer, M. *Compos. Part A.* **2005**, *36*, 345.

20. Cowan, R. D. *J. Appl. Phys.* **1963**, *34*, 926.

21. Heaney, M. B. In Electrical Measurement, Signal Processing, and Displays; Webster, J. G., Ed., CRC Press: Boca Raton, FL, **2003**, Chapter 7. p. 768.

22. Gaymans, R.; van Utteren, T.; van den Berg, J.; Schuyer, J. *J. Polym. Sci. Polym. Chem. Ed.* **1977**, *15*, 537.

23. Ramesh, C. *Macromolecules*. **1999**, *32*, 3721.

24. Atkins, E.; Hill, M.; Hang, S.; Keller, A.; Organ, S. *Macromolecules*. **1992**, *25*, 917.

25. Brill, R. *J. Prakt. Chem.* **1942**, *161*, 49.

26. Hill, M.; Atkins, E. *Macromolecules*. **1995**, *28*, 604.

27. Bermúdez, M.; León, S.; Alemán, C.; Muñoz-Guerra, S. *J. Polym. Sci. Part B: Polym. Phys.* **1999**, *38*, 41.

28. Song, Y.; Zheng, Q. *J. Appl. Polym. Sci.* **2007**, *105*, 710.

29. Derks, W.; Moonen, J.; Ramaekers, F.; Kooij, C.; Smeets, J. *Integ. Fund. Polym. Sci. Technol.* **1991**, *5*, 131.

30. Yamanobe, T.; Kurihara, Y.; Uehara, H.; Komoto, T. *J. Mol. Struct.* **2007**, *829*, 80.

31. Layachi, A.; Frihi, D.; Satha, H.; Seguela, R.; Gherib, S. *J. Therm. Anal. Calorim.* **2016**, *124*, 1319.

32. Weidenfeller, B.; Höfer, M.; Schilling, F. R. *Compos. Part A.* **2004**, *35*, 423.

33. Weidenfeller, B.; Anhalt, M.; Kirchberg, S. *J. Appl. Phys.* **2012**, *112*, 093513.

34. Ha, S. M.; Kwon, O. H.; Oh, Y. G.; Kim, Y. S.; Lee, S.-G.; Won, J. C.; Cho, K. S.; Kim, B. G.; Yoo, Y. *Sci. Technol. Adv. Mater.* **2015**, *16*, 065001.

35. Weidenfeller, B.; Anhalt, M. *J. Therm. Comp. Mater.* **2014**, *27*, 895.

36. Ren, D.; Zheng, S.; Wu, F.; Yang, W.; Liu, Z.; Yang, M. *J. Appl. Polym. Sci.* **2014**, *131*, 39953.

37. Liang, J.-Z. *Polym. Test.* **2017**, *62*, 219.

38. Traina, M.; Pegoretti, A.; Penati, A. *J. Appl. Polym. Sci.* **2007**, *106*, 2065.

39. Krupa, I.; Novak, I.; Chodak, I. *Synth. Met.* **2004**, *145*, 245.

40. Liang, J.-Z.; Yang, Q.-Q. *Adv. Polym. Technol.* **2018**, *37*, 2238.